A new laser test stand for simulating charged-particle tracks

Y. Unno[1], Y. Iwata[2], T. Ohsugi[2], T. Kohriki[1], T. Kondo[1], S. Terada[1], H. Iwasaki[1] and Y. Yamada[3]

[1]Physics Division, National Laboratory for High Energy Physics (KEK),
Tsukuba, Ibaraki 305, Japan
[2]Department of Physics, Hiroshima University,
Higashi-Hiroshima, Hiroshima 739, Japan
[3]Astro Design Co. Ltd,
Kawasaki, Kanagawa 211, Japan

ABSTRACT

We report on the construction of a new laser test stand equipped with a 1064nm pulsed infrared YAG laser for simulating the passage of a charged particle in a silicon detector. The standard semiconductor repairing tool, the so-called laser-cutter, has been modified to have a newly developed optics which has the ability to reduce the light by the order of 10^6~10^8 and to adjust the spot size to several microns. As an application we measured the position dependence of the induced signals in a silicon-strip detector when the laser light hits in the region between the strips. The measurement has shown that this device is very effective in evaluating the detailed response of a silicon detector without using charged particles generated by accelerators.

I. INTRODUCTION

Normally, in order to evaluate a silicon detector we use charged particles produced by particle accelerators [1]. It would be desirable to have alternative equipment which could perform a similar job in the laboratory [2]. A charged particle passing through silicon generates electron-hole pairs along its passage in the bulk. Laser light of 1064 nm from a YAG laser is suitable for simulating the signals generated by charged particles in a silicon detector. Since the bandgap of silicon is 1.1 eV, corresponding to a wavelength of 1130 nm, 1064 nm light has an attenuation length of about one millimeter in silicon bulk [3], and induces electron-hole pairs along the passage of the light nearly uniformly in a bulk of several hundred microns.

In the semiconductor industry the YAG laser is being used to evaporate aluminum traces on LSI chips to repair a short, or a mis-designed, trace in the chip. The laser is mounted on a microscope situated on a probe station (or prober), and is usually equipped with a collimator to limit the spot size from several tens of microns to several microns in order to evaporate the target traces. The setup is called "Semiconductor repairing equipment".

The setup is most suitable for our application of generating the signals of charged particles. Although a spot size of several microns is appropriate, the laser power is too high for this application, even though an order of magnitude of light would be lost in the collimating process. Laser power of about 50 μJ is required to evaporate a trace having a width of about 10 μm. In order to generate about 20,000 e-h pairs in the silicon bulk we require power of about 3.5 fJ. Counting losses in collimating process and quantum efficiency, we would require power of 5 pJ. Thus, a reduction on the order of about 10^7 is required. Although a low-power laser of a few 10 mW is available with a very short pulse-width of 50 ps to a nano-second, this power would be not enough to tolerate the losses in the collimating process.

If we could reduce the light power of the standard "semiconductor repairing equipment", we could use the equipment for both repairing and generating signals. We have built such reduction optics and have used the system to evaluate induced signals in a double-sided silicon-strip detector. We give in this paper a description of the reduction optics and the result of the measurement.

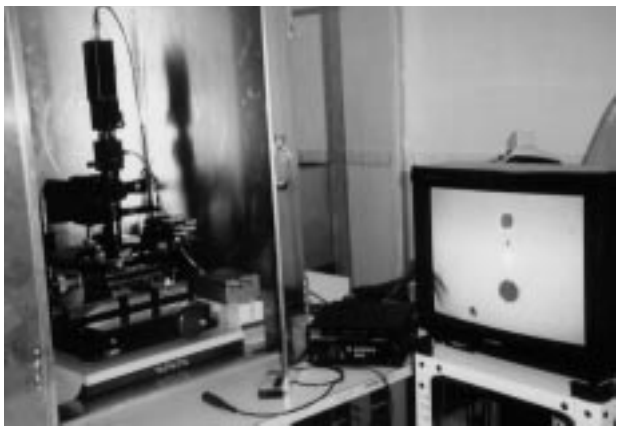

Fig. 1. Overview of the laser test stand. The prober can be seen on the left-hand side with the Nd:YAG laser at the top of the device. A monitor screen displays the object and the laser light spot.

II. SETUP

Fig. 1 shows a photograph of the prober equipped with a 1064 nm laser [4,5]. The specifications of the laser are summarized in Table 1. The microscope was equipped with Infra-Red transparent lenses and ports for the laser and for a CCD monitor [6]. A laser power-reduction unit (the laser

mounting adapter) was inserted between the microscope and the laser.

A silicon strip detector was put on an X-Y stage of the prober and moved manually. The position of the laser spot was measured on a CCD video screen. The collimation and the focus of the laser spot was also monitored on the screen.

Table 1. Specifications of the 1064-EHQ laser

Energy/Pulse	55 μJ
Wavelength	1064 nm
Gain material	Nd:YAG
Pulse width(*)	11~15 ns
Peak power(*)	3.7~5 kW
Q-switch PRF	0~25 KHz
Pulse-pulse stability	<3% rms
Beam diameter	0.5 mm
Beam divergence	<4 mrad
Polarization ratio	>100:1
Timing jitter(*)	<10 ns
Warm-up time	<15 min

(*) measured at 0~1 kHz PRF

III. THE LASER MOUNTING ADAPTER

We adopted two reduction components: ND filters and a polarizer. The major power reduction was achieved by the ND filters. A variation in the power was produced using a polarizer. The laser power could be reduced by adjusting its power supply. However, the diode-pumped YAG laser that we used had a characteristic of pulse-width widening when the pumping power was reduced. In order to keep the pulse width in the range of 10 ns, we needed to maintain the laser output at its maximum.

A schematic drawing of the adapter is shown Fig. 2. The adapter was made of: a Glan Laser Polarizer, a worm-gear with a potentio-meter for rotating the polarizer, a tilt-angle adjuster, ND filters (A, B), a mirror for the reference light, and an aperture controller. In the adapter, a reference light was introduced so that the reference and the laser light would pass through the same path so as to visually confirm the collimation and focus of the spot. Since the visual light and the laser had different wavelength, all of the optical components had to have similar characteristics for both wavelengths. The maximum transparency of the adapter was about 85%, which still enabled the laser to evaporate aluminum traces. The maximum reduction ratio was about 10^8, and was variable in the range of 10^6~10^8. Below we briefly describe the components, and summarize their specifications in Table 2.

Glan Laser Polarizer

Using the polarization of laser light, an external polarizer can control the power of laser light. The 1064-EHQ laser has a polarization ratio of >100:1. The maximum transparency of the polarizer was 92% and the maximum reduction rate was $<10^{-2}$ [7]. The polarizer could withstand a maximum laser power of 10 MW/cm^2 pulsed. The laser power was about 5kW/cm^2.

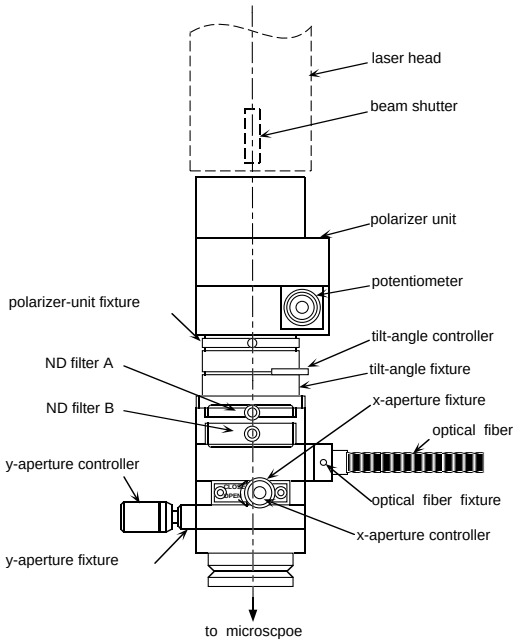

Fig. 2. Laser mounting adapter, placed between the laser head and the microscope. The reference light is introduced to this adapter.

Worm-gear with a potentio-meter

A worm-gear was attached to the Glan polarizer. The rotation was controlled by a potentio-meter connected to the gear. The polarizer rotated 90° as the potentio-meter rotated 10 times.

Tilt-angle controller

A controller was used to adjust the tilt-angle of the laser head so that the laser light hit the optics at the normal angle.

ND filters

These filters were the main power reducer. Two filters (A and B) were used in series. Each had a visible-light transparency of about 0.3%. There was no available measurement of the transparency for IR light. We assumed that the transparency for IR light was similar to that of visible light.

Mirror

A mirror combined the laser-light and the visible-light into the common optical axis. The transparency for 1064nm light

was 92%. The reflection rate was 90~92% for 600~900 nm light.

Aperture controller

Aperture controllers controlled the openings and the positions of the openings in the X and Y directions. The range of the opening was 0 to 10 mm in both directions. With the full opening the laser spot size was about 50μm in diameter. By closing the aperture the spot could be made as small as 2μm, which was eventually limited by diffraction.

Table 2. Specifications of the components of the laser mounting adapter

Glan Laser Polarizer	
Clear aperture	8 mm
Surface quality	20/10
Wavelength range	215 nm - 2.3 μm
Transparency	92 %
Reduction rate	$<1\times10^{-2}$
ND filters	
Aperture	ϕ15 mm
Transparency (visible light)	~0.3%
Mirror	
Transparency (1064nm)	92%
Reflection rate (600~900 nm)	90~92%
Aperture controller	
X-Range	0~10 mm
Y-Range	0~10 mm

Table 3. Specifications of the silicon strip detectors

	SDC prototype	SVX II test detector
Type	Double-sided	Double-sided
Coupling	AC	AC
Substrate	n-type	n-type
Chip size	60.0mm×34.1mm	78.85mm×17.12mm
Wafer thickness	300 μm	300 μm
n-side		
Strip pitch	50 μm	74.5 μm
Number of strips	640	1024
Implant strip width	12 μm	18 μm
Al strip width	6 μm	12 μm
p-isolation width	26 μm	45 μm
Bias resistor	250 kΩ	1 MΩ
Readout	Single metal layer	Double metal layer
2nd metal pitch		59 μm
p side		
Strip pitch	50 μm	60 μm
Number of strips	640	258
Implant strip width	12 μm	14 μm
Al strip width	6 μm	8 μm
Bias resistor	250 kΩ	1 MΩ
Readout	Single metal layer	Single metal layer
Stereo	10 mrad	90°

IV. APPLICATION - RESPONSE IN SILICON STRIP DETECTORS

One of our main interests in the silicon-strip detector is the hit-position dependence of signals in neighboring strips. If the signal of a strip is proportional to the distance of the hit position from the strip, the position resolution can be improved by measuring its pulse heights. The laser test stand produces a laser-beam spot of several microns, which is sharp enough for such a study with a strip pitch of 50 microns, for example.

In a silicon-strip detector with a strip pitch of several tens of microns, a large number of readout channels are packed in a small volume. To reduce the number of readout channels, a sparse-readout or a ganged-readout method are often applied. In the case of a sparse readout, every other (or, third, fourth, ...) strip is read out. In the case of a ganged readout, two (or a few) strips are ganged into one readout channel. We scanned the laser light from one strip to the other and measured the hit-position dependence of induced signals for the non-sparse (i.e., every channel), sparse, and ganged readout methods with the laser test stand.

Two types of silicon-strip detectors were tested: a double-sided silicon-strip detector with a single metal-layer readout and a double-sided detector with a double metal-layer readout. The former was an SDC prototype detector [8] and the latter was a test detector for the SVX II [9]. Their specifications are briefly listed in Table 3.

Hit-position dependence of signals

The spot positions and raw induced signals are shown in Fig. 3. The laser light, with a spot size of 3 μm × 3 μm (at the top surface), was scanned over the n-side of the SDC prototype silicon-strip detector. The divergence of the laser light was about 100 mrad. The distances between the readout strip and the laser spots are indicated in the figure. In the measurement, only one strip was connected to a readout electronics [10] and the neighboring strips were floated. The integration time of the electronics was of order of μsec. The detector was reverse-biased at 85 V, while the full depletion voltage of the detector was 75 V. The intensity of the laser was adjusted so that the same order of the output was obtained as that of beta rays from ^{90}Yttrium. There was no signal when the laser spot hit the readout electrode. This was proof that the laser spot size was smaller than the strip width (6μm). From these observations we could say that the nearer was the hit the larger was the induced signals. We should note, however, that the measurement was performed for the case where neighboring strips were floating, resulting that the pulse heights in Fig. 3(e) and Fig. 3(f) were the same.

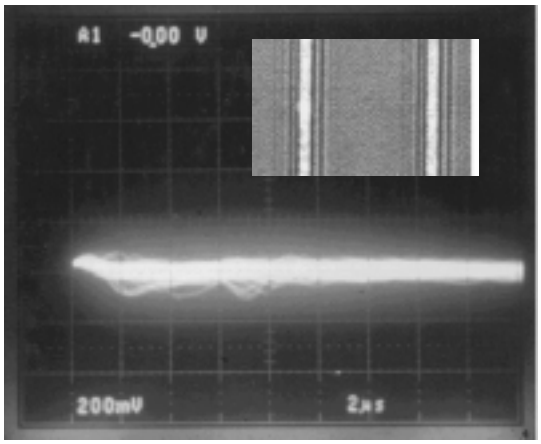

(a) 0 μm

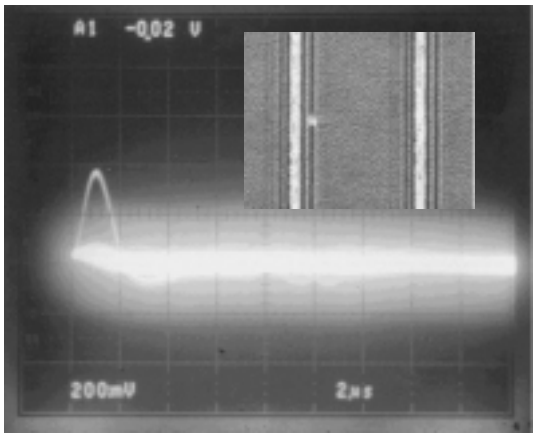

(b) 5 μm

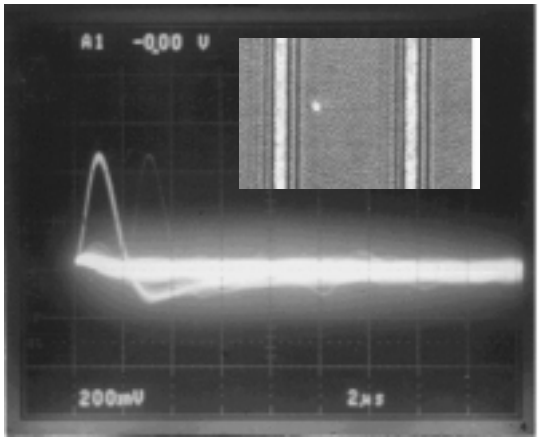

(c) 10 μm

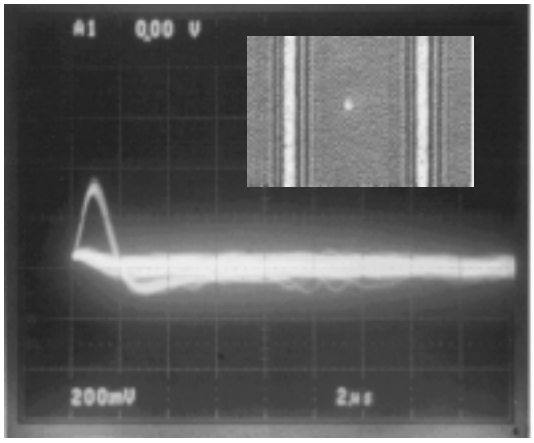

(d) 20 μm

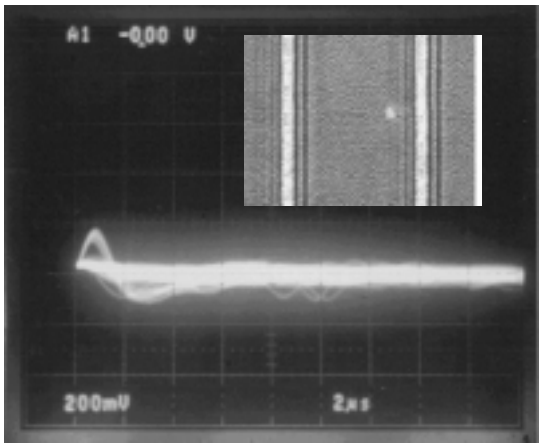

(e) 35 μm

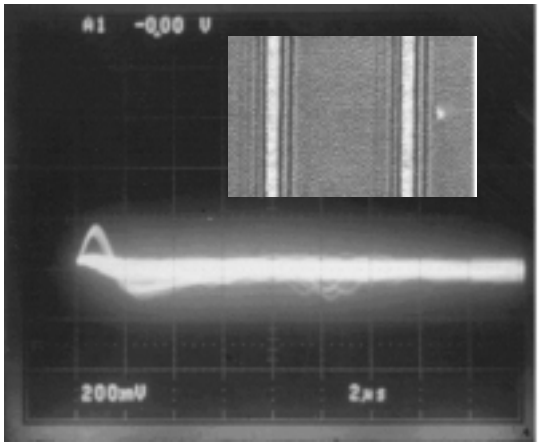

(f) 60 μm

Fig. 3. Spot positions of the laser light on the SDC prototype silicon strip detector and the induced signals at the n-side on the oscilloscope. The spot size was 3 μm by 3 μm. The inset figures show the readout strips and the spot. The strip pitch was 50 μm and the left-hand side strip was the readout. Spot from the readout at, (a) 0 μm, (b) 5 μm, (c) 10 μm, (d) 20 μm, (e) 35 μm, and (f) 60 μm.

Fig. 4 (a) and (b) show the pulse-height distributions as a function of the position. In these measurements, two successive strips were read out while the electrodes outside of these two strips were grounded. The origin of the abscissa was defined at the left edge of the left-side readout aluminum strip. The signals were not linear to the distance from the readout strip. There were steps at the middle point of the strips, where the electric-field lines were separated so as to go to the respective implant strips. The steps were clearer for signals of the p side (i.e., junction-side) than for that of the n side. A further study of the electric field in the bulk, the charge collection, and an investigation of the optics of the laser light, i. e. focus, defocus and attenuation in the bulk, are necessary in order to understand the difference between these steps in detail.

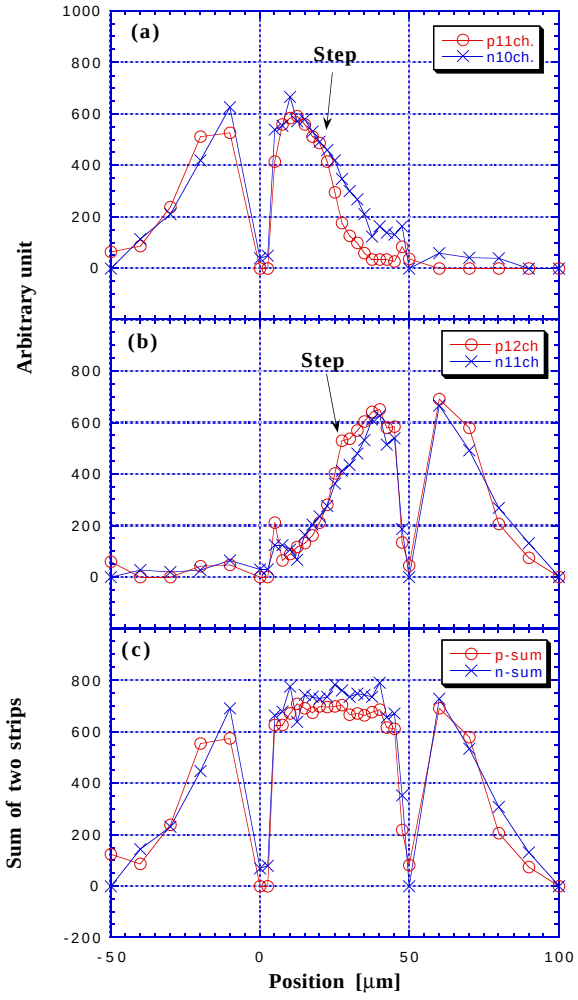

Fig. 4. Hit-position dependence of signals to the laser light in the p- (circle) and n-side (cross) of the SDC double-sided single-metal-layer detector. Two successive strips were read out while aluminum electrodes of the neighboring strips were grounded: (a) one readout channel, (b) next readout channel, (c) sum of the two channels with software.

When the laser spot hit more distant positions over the neighboring strip, there was essentially no signal in the readout strip, in contrast to the Fig. 3. The signal was shielded by the neighboring strip, since it was grounded. A sum of the signals in the two strips were made with software and is plotted in Fig. 4 (c). The sum was essentially uniform between the two readout channels.

Sparse readout and ganged readout

For a sparse readout, two strips were connected to readout electronics with one intermediate strip being unconnected in the SDC detector. The center strip is the so-called "floating intermediate" strip. The signal pulse heights are shown in Fig. 5, for (a) one readout channel, (b) next readout channel, and (c) a sum of the two channels being added with software. In the scanning, the origin of the position was defined as being at the left edge of the intermediate aluminum strip. Four regions (-50 μm to -25 μm, -25 μm to 0 μm, 0 μm to +25 μm and +25 μm to +50 μm) showed different characteristics in the p-side. There were signals in the readout strip when the laser light hit the region beyond the floating strip, similar to that shown in the Fig. 3. At the p-side, there was a large signal in the first region (the nearest region to the readout strips). The signals were almost flat in the second and third regions. They were about 1/3 and 1/4 of the maximum signal in the first region, respectively. In the fourth region it was diminishing. At the n-side, however, the signals looked to be proportional to the distance from the readout strip.

As clearly seen in the sum of the two channels, the observed charges around the intermediate strip were smaller than the charges observed around the readout strips. Since no amplifier was connected to the intermediate strip, charges collected in the intermediate strip were coupled to the neighboring readout strips capacitively. The less charges in the intermediate strip indicated that there were other capacitively coupled regions, such as the backplane and other adjacent strips from the intermediate strip. The amplifier integration time of μsec was much slower than the charge collection time of order of 10 ns; no ballistic deficit was involved.

The sparse and ganged-readout methods were also investigated in the n-side of the SVX II detectors. The detector had a double-metal-layer structure on the n- (ohmic) side. A bias voltage of 80 V, which was 20 V higher than the full-depletion voltage, was applied. The resulting pulse-height distributions are shown in Fig. 6. In the sparse readout, the strip at 0 μm was floated. In the ganged readout, the strips at -75 μm and 0 μm, and the strips at +75 μm and +150 μm were ganged.

In the sparse readout, the signals were about 1/6 of the maximum near to the intermediate strip, which were much lower than those in the case of the SDC detector. The SVX II detector had a double-metal structure and a larger interstrip capacitance (10 pF) compared with that of the SDC single

metal structure (7 pF) even though the strip pitch (74.5 μm) was larger than that (50 μm) of the SDC detector. These structural parameters may have caused a difference in the signals. With the low pulse heights and non-linearity, we can not expect a good efficiency nor a better resolution than that of the readout pitch in the sparse readout of the SVX II detector.

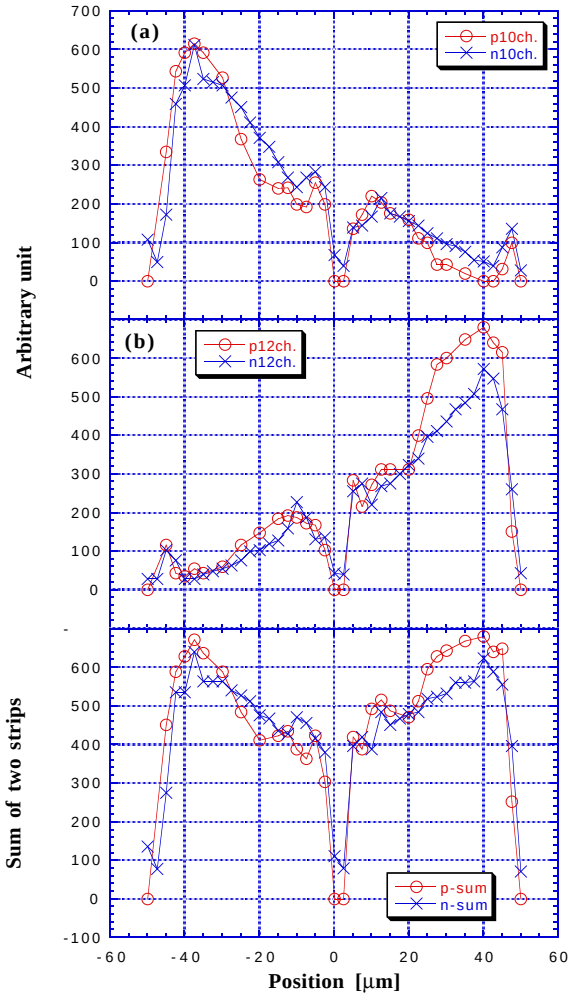

Fig. 5. Signals in the sparse readout with one intermediate floating strip (p-side (circle) and n-side (cross)). The origin of the position was at the left edge of the intermediate aluminum strip: (a) one readout channel, (b) next readout channel, (c) a sum of the two channels with software.

In the ganged readout, the laser light hit two regions: the region inside the ganged pair, and the region between the readouts. The signals inside the ganged pair were large and flat in position. The signals between the readouts gradually decreased as the laser spot hit further from the readout strip. In this region, the sums of two signals in the two readouts were equal to the signals of the spot inside the ganged pair. From these observations we could expect a higher efficiency for the ganged readout than that of the sparse readout.

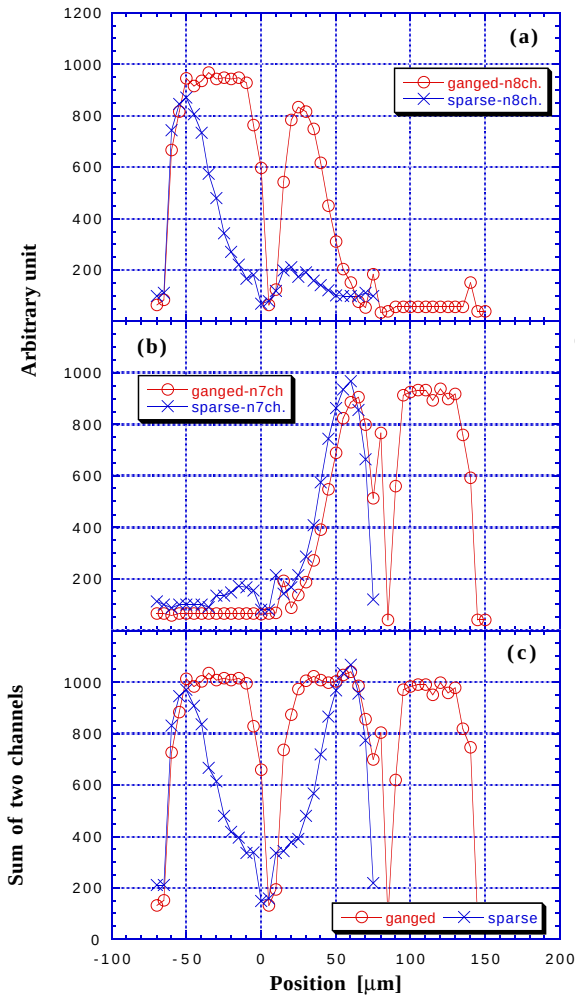

Fig. 6. Signals in the sparse readout (cross) and the ganged readout (circle) at the n- (ohmic) side of the SVX-II prototype double-metal-layer detector: (a) one readout channel, (b) other channels, and (c) a sum of the readout channels with software. In the sparse readout, the strip at 0 μm was floated. In the ganged readout, the strips at -75 μm and 0 μm, and the strips at +75 μm and +150 μm were ganged.

V. SUMMARY

We have built a laser test stand which simulates the response to charged particles for characterizing silicon-strip detectors. A modification was made to semiconductor repairing equipment with a pulsed Nd:YAG laser having a wavelength of 1064 nm. Special effort was made to reduce the power of the laser light to be on the order of 10^6 to 10^8, with filters and a polarizer, and to make a small light spot on the order of several microns. The laser test stand has worked not only as a detector test stand but also as an original

repairing tool when the filters are removed and the polarizer is set at the maximum transparency.

We have applied the laser test stand to investigate the hit-position dependence of induced signals in silicon-strip detectors with strip pitches being on the order of tens of microns. Signals were generated by shinning laser light between the strips. We have observed a similarity and a difference in response at the p-side and the n-side with non-sparse and sparse readout (with one intermediate strip). We have taken quantitative data for two kinds of double-sided silicon-strip detectors: a single metal-layer detector and a double metal-layer detector, with a sparse readout (with one intermediate strip) and a ganged readout in detail. The double metal structure has shown very low pulse heights near and over the intermediate strip in the sparse readout.

The results given in this paper have demonstrated the good performance of this test stand and a quick characterization of silicon detectors without charged particles from accelerators.

REFERENCES

[1] Y.Unno et al., "Beamtests of the double-sided silicon strip detectors with fast binary readout electronics", International Symp. on Development and Application of Semiconductor Tracking Detectors at Hiroshima, Oct. 10-13, 1995.

[2] B.S. Avset et al., Nucl. Instr. and Meth. A310(1991)203; E. Barberis et al., The Fermilab Meeting DPF92, C.H. Albright ed. (World Scientific, Singapore 1992), Vol 2, p1752; S. Gadomski et al., Nucl. Instr. and Meth. A326(1993)239; K. Ing et al., Nuc. Scie. Symp., 1994 IEEE Conf. Rec. p510.

[3] H.Melchior, "Demodulation and Photodetection Techniques," in F.T.Arecchi and E.O.Schulz-Dubois, Eds., Laser Handbook, Vol. 1, North-Holland, 1972, pp725-835

[4] Manual Prober Model SE-6001, ASTRO Design, Inc., 863 Kamikodanaka, Nakahara-ku, Kawasaki-shi, Kanagawa 211, Japan

[5] ALC Q-Switched Microlaser, Model 1064-EHQ with programmable laser controller 120894, Amoco Laser Company, 1251 Frontenac Road, Naperville, IL 60563, U.S.A.

[6] Model VMU-3H, Mitsutoyo Co. Ltd.

[7] Tower Optical Corporation, Wayne, New Jersey 07470, U.S.A.

[8] T. Ohsugi, et al. Nucl. Instr.and Meth. A342(1994)16.

[9] D. Bortoletto, S. Seidel, J. Spalding, International Symp. on Development and Application of Semiconductor Tracking Detectors at Hiroshima, Oct. 10-13, 1995.

[10] Hybrid charge-sensitive preamplifier, Model N012-1, Hoshin Densi Co. Ltd., Hatanodai, Shinagawa, Tokyo 142, Japan, and a spectroscopy amplifier, Model 472, EG&G ORTEC, Oak Ridge, TN 37831-0895, U.S.A.